ORIGINAL RESEARCH

Electroacupuncture Pretreatment at Zusanli (ST36) Ameliorates Hepatic Ischemia/Reperfusion Injury in Mice by Reducing Oxidative Stress via Activating Vagus Nerve-Dependent Nrf2 Pathway

Haochen Jiang[1,2,*], Zhi Shang[2,*], Liping You[1,2,*], Jinghao Zhang[1], Junzhe Jiao[2], Yihan Qian[2], Jiacheng Lin[2], Fang Wang[2], Yueqiu Gao[1], Xiaoni Kong[2], Xuehua Sun[1]

[1]Department of Liver Diseases, Shuguang Hospital Affiliated to Shanghai University of Traditional Chinese Medicine, Shanghai, People's Republic of China; [2]Central Laboratory, Shuguang Hospital Affiliated to Shanghai University of Traditional Chinese Medicine, Shanghai, People's Republic of China

*These authors contributed equally to this work

Correspondence: Xuehua Sun, Department of Liver Diseases, Shuguang Hospital Affiliated to Shanghai University of Traditional Chinese Medicine, Shanghai, People's Republic of China, Email susan_sxh@shutcm.edu.cn; Xiaoni Kong, Central Laboratory, Shuguang Hospital Affiliated to Shanghai University of Traditional Chinese Medicine, Shanghai, People's Republic of China, Email xiaonikong@shutcm.edu.cn

Background and Purpose: Current pharmacological approaches to prevent hepatic ischemia/reperfusion injury (IRI) are limited. To mitigate hepatic injury, more research is needed to improve the understanding of hepatic IRI. Depending on traditional Chinese medicine (TCM) theory, acupuncture therapy has been used for the treatment of ischemic diseases with good efficacy. However, the efficacy and mechanism of acupuncture for hepatic IRI are still unclear.

Methods: Blood provided to the left and middle lobe of mice livers was blocked with a non-invasive clamp and then the clamps were removed for reperfusion to establish a liver IRI model. Quantitative proteomics approach was used to evaluate the impact of EA pretreatment on liver tissue proteome in the IRI group. Serum biochemistry was used to detect liver injury, inflammation, and oxidative stress levels. H&E staining and TUNEL staining were used to detect hepatocyte injury and apoptosis. Immunohistochemistry and ELISA were used to detect the degree of inflammatory cell infiltration and the level of inflammation. The anti-inflammatory and antioxidant capacities were detected by Quantitative RT-PCR and Western blotting.

Results: We found that EA at Zusanli (ST36) has a protective effect on hepatic IRI in mice by alleviating oxidative stress, hepatocyte death, and inflammation response. Nuclear factor E2-related factor 2 (Nrf2) as a crucial target was regulated by EA and was then successfully validated. The Nrf2 inhibitor ML385 and cervical vagotomy eliminated the protective effect in the EA treatment group.

Conclusion: This study firstly demonstrated that EA pretreatment at ST36 significantly ameliorates hepatic IRI in mice by inhibiting oxidative stress via activating the Nrf2 signal pathway, which was vagus nerve-dependent.

Keywords: inflammation, liver, proteomics

Introduction

Ischemia-reperfusion injury (IRI) refers to the occurrence of ischemia or hypoxia in human organs or tissues. Restoring blood and oxygen supply not only fails to restore, but also aggravates the damage of organs or tissues, including the liver, kidneys, gastrointestinal tract, and many other organs.[1] Hepatic IRI is important for surgical operations, which greatly affects the success rate of surgery and the occurrence of complications.[2]

Oxidative stress is a pathological condition of tissue damage caused by overproduction, or a reduction in the ability to scavenge reactive oxygen species (ROS).[3] An excessive amount of ROS causes oxidative stress, which starts inflammation. As a key regulator of oxidative stress, Nrf2 prevents cells from oxidative stress via antioxidant enzymes. A potent

1595

Nrf2 activator, CDDO-imidazoline, improved hepatic IRI by activating the Nrf2 downstream gene leading to reduce ROS production and inflammatory response.[4]

Current pharmacological methods to prevent and treat hepatic IRI are limited. Therefore, more research is needed to improve the understanding of hepatic IRI and to find methods that can mitigate damage. Acupuncture therapy is used throughout all aspects of theory of traditional Chinese medicine (TCM). Electroacupuncture (EA) is a method of stimulating acupuncture points by applying pulsed electrical currents to acupuncture needles and is widely used in the clinical treatment of various diseases. A growing body of reports have shown the protective impact of EA against IRI.[5,6] The ancients believed that problems in the internal function of the viscera would be reflected on the body's surface and that treatment or relief of discomfort could be achieved by stimulating the reaction points on or under the skin, and the target of such stimulation was the acupuncture point. One of the most commonly used acupuncture points is the Zusanli (ST36), located at four finger widths from the lower edge of the kneecap, and one finger width lateral to the anterior tibial crest, which has excellent anti-inflammatory, antioxidant and recovery properties.[7,8] In mice, it is located at the tibialis anterior, about 1/6 of the way between the patella and the lateral malleolus. Whether in clinical treatment effects, such as gastroscopy,[9] constipation,[10] gastric cancer;[11] or in animal experiments, such as Parkinson's disease,[12] asthma,[13] and acute renal,[14] ST36 is a widely used acupuncture point with very good therapeutic effects and research significance.

Nrf2 is a transcription factor that regulates the glutathione and thioredoxin antioxidant systems in terms of transcription.[15,16] Numerous types of research have indicated that the susceptibility to liver injury is increased in the absence of Nrf2.[17,18] And activation of the Nrf2 in ischemia-reperfusion models of the brain, kidney as well as liver attenuates IRI.[19–21] All of these suggest that Nrf2 can act as a hepatoprotective pathway.

The liver is connected to the brain through a complex neural network, and the vagus nerve, a branch of the liver, plays a very important role in regulating hepatic circulation and glucose metabolism. The vagus nerve of the liver branch can regulate the phagocytic activity of Kupffer cells and promote the regenerative and anti-inflammatory capacity of the liver.[22] In a study of liver regeneration, vagotomy (VNX) demonstrated that the vagus nerve of the hepatic branches could lead to liver regeneration and the ensure survival.[23] These suggested that the vagus nerve was also very important in the regulation of hepatoprotection.

In this research, we found that EA at ST36 pre-treatment had a significant protective effect in a model of IRI with mice. Quantitative proteomics study showed that EA inhibits oxidative stress by activating Nrf2. Further studies had shown that activation of Nrf2 by EA relates to the intact cervical vagus nerve. The mechanism of EA at ST36 to alleviate hepatic IRI has important clinical significance, providing a potential strategy to reduce the degree of IRI in liver surgery and improve the success rate of surgery.

Methods
Mice
Male C57BL/6 mice (8–10 weeks old) were obtained from Shanghai JieSiJie Laboratory Animal Co.Ltd. (Shanghai, China). All procedures involving animals were approved and performed in accordance with the Animal Care and Use Committee of Shanghai University of Chinese Traditional Medicine. Mice were housed in a room that maintained a constant humidity/temperature and were free to eat and drink.

Experimental Design
Three independent experiments were conducted in this study, using a total of 65 mice.

In the first experiment, we investigated the protective effect of electroacupuncture and screened for an optimal stimulation intensity. Mice were randomly divided into the Sham group, IRI group, IRI+NAcuP group (none acupuncture point), IRI +SEA group (acupuncture without electrical stimulation), and IRI+EA group (electroacupuncture at ST36). In the second experiment, ML385 (MedChemExpress, USA, HY-100523), an inhibitor of Nrf2, was used to explore Nrf2 as a key target for EA to improve hepatic IRI. One hour before modeling, mice were injected intraperitoneally with ML385 (30 mg·kg^{-1}). Mice were randomly divided into four groups: IRI group, IRI+ML385 group, IRI+EA group, and IRI+ML385+EA group. In the third experiment, vagotomy (VNX) was used to explore the role of the vagus nerve in electroacupuncture modulation of

Nrf2 to produce hepatoprotection. Vagotomy was performed three days before modeling to give the mice sufficient time to recover. Mice were randomly divided into four groups: IRI group, IRI+VNX group, IRI+EA group, and IRI+VNX+EA group. Serum biochemistry, Western blotting, ELISA, quantitative real-time PCR, and HE were used to observe the degree of liver injury, inflammation level, and oxidative stress level in each group.

Electroacupuncture (EA)

The operation was as previously described,[24] and the electrical stimulation intensity was set to the observable muscle twitch. EA was conducted on Zusanli (ST36) at a frequency of 2/100Hz and an intensity of 0.5 mA for 15 min per day for 6 days. A couple of acupuncture needles with a measurement of 0.16 millimeters in diameter and 7 millimeters in length (0.16·7 mm, Luoya Shanchuan Medical Device Co., Ltd., China) were inserted to a depth of 3 mm into the muscle layer at both ST36. ST36 is located on the anterior tibial muscle, about 1/6 of the way between the patella and the lateral malleolus. Electrical stimulation was provided by a HANS-200A acupoint nerve stimulator. This nonacupoint is not mentioned in the rodent acupuncture chart and is located 3 cm distal to the acupoint above the knee. Acupuncture needles with no electrical stimulation at ST36 as the SEA group. The IRI +NAcuP group and IRI+EA group only have different stimulation positions.

Mouse Liver IRI Model

The 70% warm liver ischemia/reperfusion model was established as we described earlier.[25] Pentobarbital sodium was used to anesthetize mice intraperitoneally at $100mg \cdot kg^{-1}$. Then, blood provided to the left and middle lobe of the liver was blocked with a non-invasive clamp for 90 minutes, resulting in 70% hepatic ischemia, and the success of ischemia was determined by changes in liver color. Those in the Sham groups did not have a vascular clamp applied to their veins. After ischemia, the clamps were removed for reperfusion for another 6 hours. Liver and serum samples were stored for analysis when mice were sacrificed after reperfusion. All mice were sacrificed by sodium pentobarbital solution. In our experiments, each group comprised 5 mice.

Serum Biochemistry Assay

Blood samples were collected after letting them stand at ambient temperature for at least 30 min and centrifuged at 3000 rpm for 15 min. Expression levels of alanine aminotransferase (ALT) were measured by ALT kit (Nanjing Jiancheng Bioengineering Institute, Nanjing, China, C009-2-1), and those of aspartate aminotransferase (AST) were measured by AST kit (Nanjing Jiancheng Bioengineering Institute, Nanjing, China, C010-2-1). Malondialdehyde (MDA) and superoxide dismutase (SOD) activities were detected using MDA (Shanghai Lanchu Biotechnology Co., Ltd., E-BC-K025-M) and SOD (Shanghai Lanchu Biotechnology Co., Ltd., E-BC-K022-M) assay kits, respectively. All the experimental manipulations were performed according to the manufacturer's procedure.

H&E Staining and Immunohistochemistry (IHC) Analyses

Liver tissue was fixed in 4% paraformaldehyde for 24 hours, and paraffin-embedded hepatic tissue specimens were cut into segments (5μm) according to standard procedures. Hematoxylin and eosin (H&E) were then used to stain liver sections. For immunohistochemical analysis, neutrophils were evidenced in paraffin sections using antibodies against myeloperoxidase (MPO) and F4/80.

TUNEL Staining

TUNEL staining was performed with an In-Situ Cell Death Detection Kit (Beyotime Institute of Biotechnology, China, C1090) as directed by the manufacturer.

Quantitative RT-PCR

Based on the manufacturer's instructions, liver tissues were extracted for total RNA, and cDNA was synthesized using the total RNA rapid extraction kit (BioTeke, China, RP4002). The target genes' expression levels were defined by

quantitative real-time RT-PCR using the SYBR RT-PCR kit (Vazyme, China, Q711-02). Primers used for RT-PCR analysis are:

β-actin forward: 5´- GTGACGTTGACATCCGTAAAGA
β-actin reverse: 5´- GCCGGACTCATCGTACTCC
IL-6 forward: 5´- GCTACCAAACTGGATATAATCAGGA
IL-6 reverse: 5´- CCAGGTAGCTATGGTACTCCAGAA
TNF-α forward: 5´- TTCTATGGCCCAGACCCTCA
TNF-α reverse: 5´- TTTGCTACGACGTGGGCTAC
IL-1β forward: 5´- TGTAATGAAAGACGGCACACC
IL-1β reverse: 5´- TCTTCTTTGGGTATTGCTTGG
Nrf2 forward: 5´- TCTTGGAGTAAGTCGAGAAGTGT
Nrf2 reverse: 5´- GTTGAAACTGAGCGAAAAAGGC
HO1 forward: 5´- AAGCCGAGAATGCTGAGTTCA
HO1 reverse: 5´- GCCGTGTAGATATGGTACAAGGA
NQO1 forward: 5´- AGGATGGGAGGTACTCGAATC
NQO1 reverse: 5´- AGGCGTCCTTCCTTATATGCTA

Western Blot

Collection of total protein from liver tissue using RIPA followed by determination of protein concentration (5 ug/uL) using a BCA Protein Assay Kit (Thermo Fisher Scientific) as described before.[26] Nuclear proteins from the liver were collected using Nuclear and Cytoplasmic Extraction Reagents (Beijing Full Gold Biotechnology Co., Ltd., DE201-01). The primary antibodies against F4/80, MPO, P-NF-κb, NF-κb, P-IκBα, IκBα, Nrf2 (Cell signaling technology, 70076, 14569, 3033, 8242, 2859, 4812, 12721), β-Actin (ABGENT, AP14779b), HO-1, NQO-1, Lamin B2 (Abmart, T55113, T56710, T57109) were used.

Enzyme-Linked Immunosorbent Assay (ELISA)

IL-6, TNF-a, and IL-1β were detected using mouse cytokine ELISA kits (NeoBioscience Technology, China, EMC004.96, EMC102a.96.10, EMC001b.96) according to the manufacturer's protocol.

Sample Preparation for Label-Free Proteomics

The preparation of samples was performed as previously described.[27] Perfused liver tissue was homogenized in RIPA lysis buffer to obtain total protein. After centrifugation at 4°C and 12,000 g for 10 min, a BCA Protein Assay Kit was used to measure protein concentrations that were obtained from supernatants. The reduction of 100μg of protein samples was performed at 60°C for 60 minutes using 20 mM dithiothreitol (DTT, Sigma-Aldrich), followed by alkylation with 100 mM iodoacetamide for 40 min at room temperature. Five times the volume of acetone was added, and precipitation of alkylated protein at −20°C was performed overnight. Reconstituted protein precipitates were digested all night with trypsin at a 1:50 ratio of tryptic protein volume with 100 mm ammonium bicarbonate. Finally, the peptides were desalted, vacuum-dried, and reconstituted.

LC-MS/MS Analysis and Bioinformatics Analysis

These peptides were assayed by Liquid chromatography-tandem mass spectrometry (LC-MS /MS) technique on a Q ExactiveTM HF-X (Thermo Fisher Scientific) in combination with an EASY-nLC 1000 UPLC system (Thermo Fisher Scientific). MS1 was set to 70,000 resolutions, then MS/MS was selected, and NCE was set to 28. MS2 resolution was set to 17,500. Quantitative data were analyzed by MaxQuant (v1.6.1.2) with MS/MS spectral original data to retrieve the UniProtKB mouse database (release number 2021_04, 17,090 entries) and linked to the reverse decoy database. Two missing oval cleavages were made up by using trypsin/P as an oval cleavage enzyme. The mass tolerance of the precursor ion was adjusted to 20 ppm for the First search and 6 ppm for the Main search, respectively, and the mass tolerance of the fragment ion was set to 0.02 Da. Carbamidomethylation of cysteine was defined as a fixed modification,

while for database searches, N-terminal acetylation of proteins and methionine oxidation were classified as variable modifications. The maximum FDR for peptides and proteins was set to 1% by using the reverse database strategy calculation. The intensity-based absolute quantification (iBAQ) method was used for label-free quantification. The expression of the protein was compared to each sample using normalized iBAQ values based on at least two distinct peptides and aligned for data processing. A 1.5-fold cut-off was established to screen for proteins that were differentially expressed. Differentially expressed proteins of quantitative data were submitted to Ingenuity Pathway Analysis (IPA, QIAGEN, Redwood City, http://www.ingenuity.com/), and used for protein-protein interaction analysis. P-value < 0.05 was considered to be statistically significant.

Vagotomy

Mice were gas anesthetized and placed on the operating table to maintain anesthesia. The mice were subjected to cervical left vagus nerve dissection. The procedure is as follows: remove hair from the neck, sterilize the mouse with alcohol, incise the skin and muscle to reveal the left cervical vagus nerve, then gently separate the vagus nerve with a glass needle, avoiding damage to the blood vessels and ensuring that the nerve is cut and excised with scissors for at least 1 cm. Subsequently, the mouse neck muscle and skin were sutured sequentially according to the suture criteria.

Statistical Analysis

GraphPad Prism 8.0 software was used for data analysis. All data were presented as the means ± SD. The number of animals is determined based on the results of preliminary experiments. To compare variables among groups, statistical analyses were performed using one-way ANOVA test or two-tailed Student's *t*-test as appropriate. $P < 0.05$ was considered statistically significant.

Results

Electroacupuncture Stimulation on the ST36 Protected Mice from Hepatic IRI

Previous studies have shown that EA can reduce damage led by IRI.[5,28] To assess the impact of EA on hepatic impairment caused by ischemia-reperfusion, we pre-treated mice with EA. The experimental design was shown in Figure 1A. Consistent with previous studies, acupuncture without electrical stimulation of the ST36 had a significant therapeutic effect on liver IRI, and this therapeutic effect was even more significant after EA. However, the expected therapeutic effect could not be achieved when EA was performed at non-acupoints, indicating the specific role of ST36 under EA. The results revealed that EA intervention on the ST36 attenuated hepatic injury after ischemia/reperfusion, as the level of serum ALT and AST were highly declined in the EA group than IRI group (Figure 1B and C). Some studies had shown that the effect is better than acupuncture because of the continuous stimulation by EA.[29] Usually, in clinical practice, the doctor treats the patient with acupuncture, increasing the amount of stimulation at regular intervals by lifting and twisting the needle handle to achieve a sustained effect. However, regular electrical stimulation by EA can compensate for manual operation. IRI directly leads to severe necrosis in the liver. We also found an obvious improvement in liver morphology of the EA group, and the hepatic necrosis area in the EA group was smaller than IRI group (Figure 1D). To analyze the protective effect of EA on hepatocytes, we performed TUNEL staining. The results showed that hepatocyte apoptosis dramatically increased after IRI. However, the EA pre-treatment could significantly reduce hepatocyte death compared with the IRI group (Figure 1E). Collectively, the results demonstrated that EA on the ST36 could effectively reduce hepatic IRI by protecting hepatocytes from death.

EA Stimulation on the ST36 Alleviated Inflammatory Responses and NF-κb Pathway Activation in Mice Hepatic IRI

As we know, IRI causes inflammation and ROS generation, resulting in cell death.[30] We, therefore, assessed the impact of EA on inflammatory responses. Our data show that EA pre-treatment on the ST36 significantly inhibited the level of proinflammation cytokines in liver tissues of IRI mice, including TNF-α, IL-6, and IL-1β (Figure 2A–C).
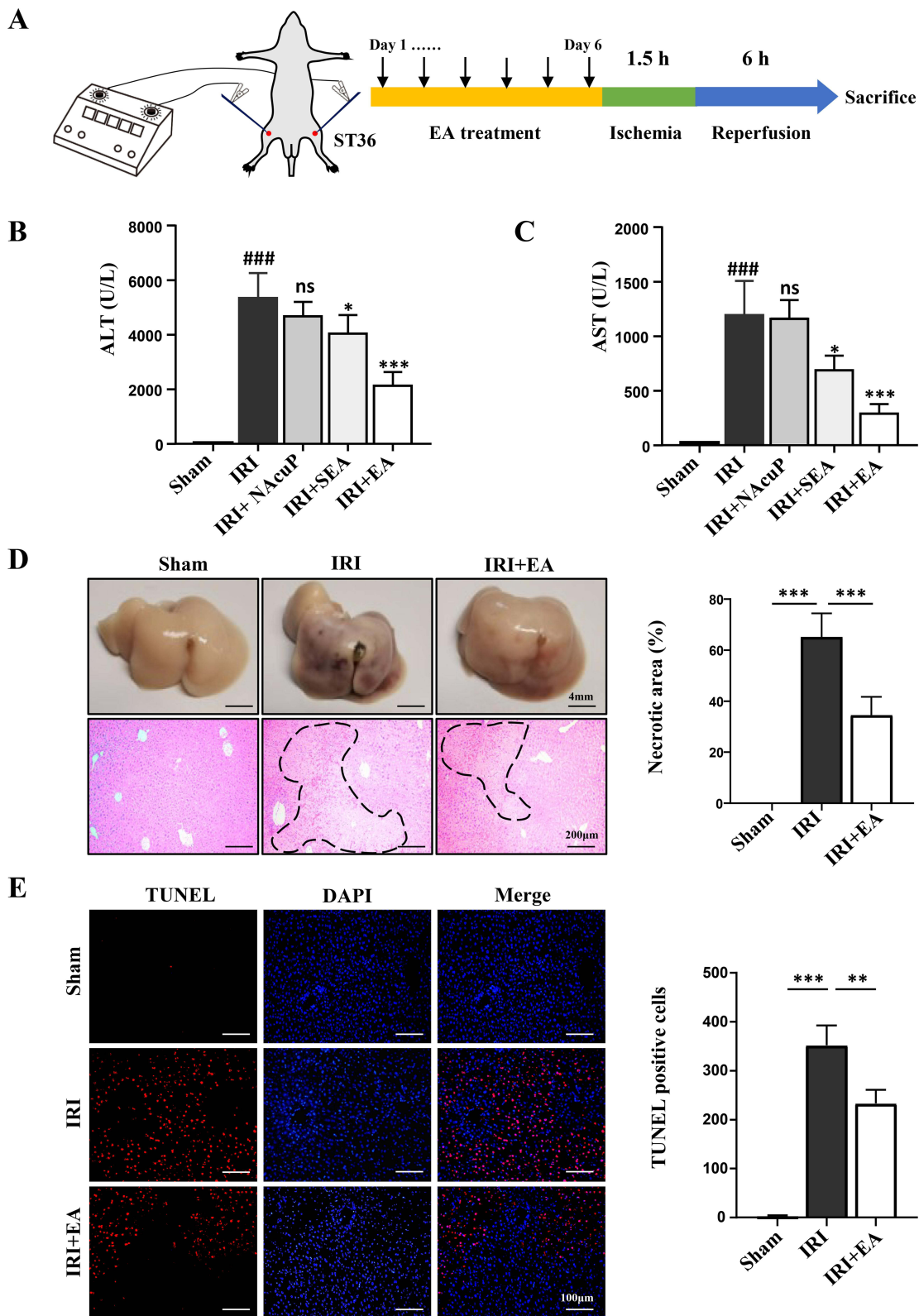
Figure 1 EA ameliorated hepatic IRI injury. (**A**) The experimental design. (**B** and **C**) ALT and AST levels using different stimulation methods. (**D**) Representative HE images of liver tissues (original magnification, × 100) showed necrotic areas. (**E**) TUNEL-positive cells were examined using TUNEL staining for TUNEL (red) and DAPI (blue). The TUNEL-positive hepatocytes were shown. All data were shown as the mean ± SD. $^{\#}P < 0.05$, $^{\#\#}P < 0.01$, $^{\#\#\#}P < 0.001$ compared with the Sham group, $^{*}P < 0.05$, $^{**}P < 0.01$, $^{***}P < 0.001$, compared with the IRI group (n = 5 per group).
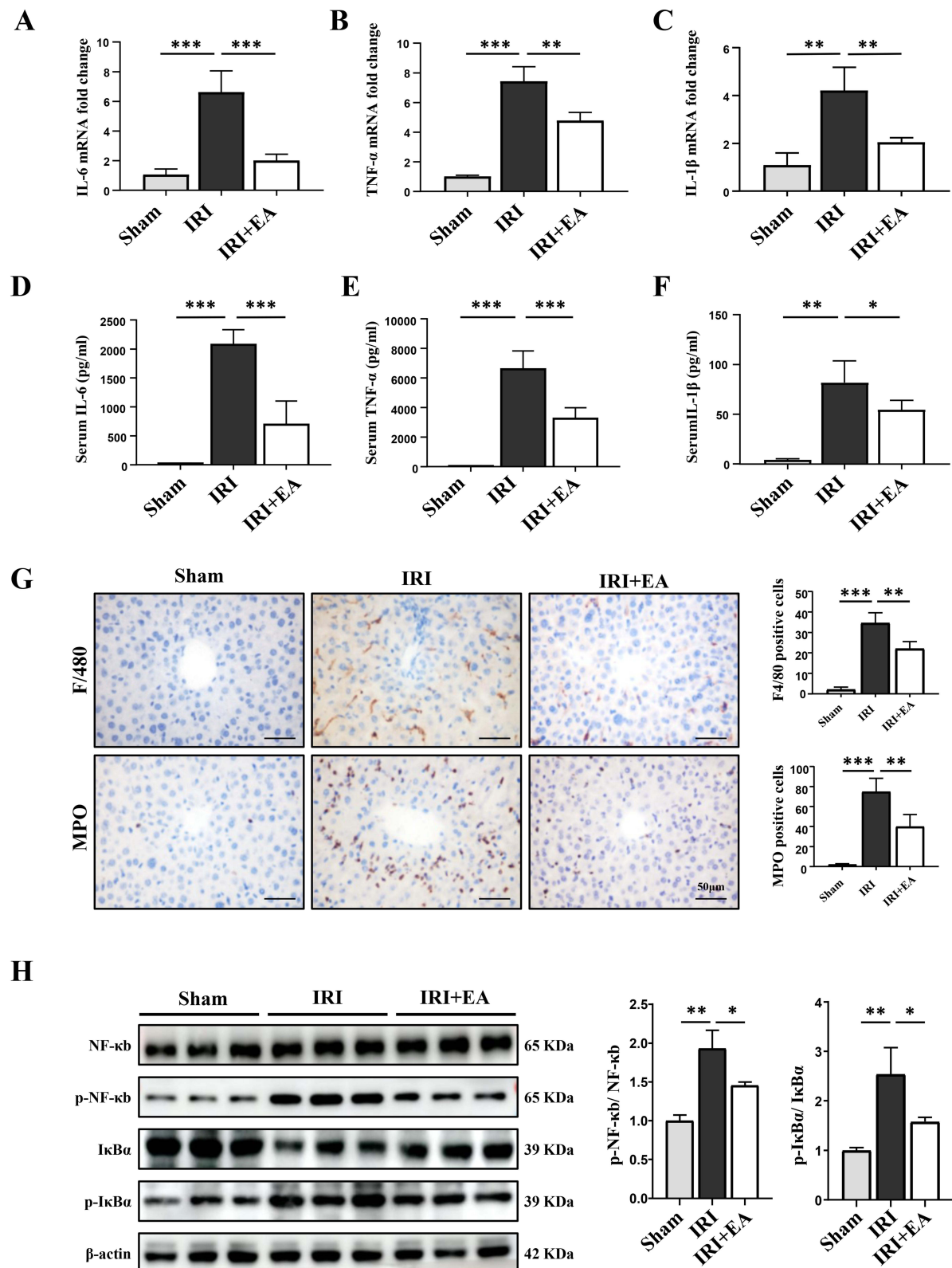
Figure 2 EA alleviated inflammatory responses in mice hepatic IRI. (**A–C**) The mRNA levels of IL-6, TNF-α and IL-1β. (**D–F**) Serum levels of indicated cytokines were measured by ELISA. (**G**) F4/80 and MPO staining in liver tissue sections (original magnification, × 400) and the positive cells. (**H**) NF-κb, p-NF-κb, IκBα and p-IκBα expression in the liver tissues were measured by Western blot (n=3 per group). β-actin was used as a loading control. All data were presented as the mean ± SD. *P <0.05, **P < 0.01, ***P < 0.001 (n=3–5 per group).

The same results were also observed in serum samples by ELISA (Figure 2D and E). IHC was executed to observe hepatocyte infiltration of immune cells, including MPO (a marker for neutrophils) and F4/80 (a marker for macrophages). The infiltration of neutrophils and macrophages in liver tissue was reduced in the IRI+EA group than IRI group (Figure 2G). We examined the expression levels of NF-κb, p-NF-κb, IκBα, and p-IκBα, which all belong to the NF-κb signal pathway, to further validate the above-observations. Ischemia-reperfusion significantly increased the phosphorylation level of IκBα, causing NF-κb activation, then inducing inflammation. However, after EA treatment, the level of p-IκBα and p-NF-κb were greatly decreased than the IRI group, and the data revealed that EA treatment suppressed NF-κb signal pathway activation, resulting in inhibiting the inflammatory responses (Figure 2H).

Quantitative Proteomics Analysis Revealed EA Stimulation Significantly Inhibited Oxidative Stress

Based on LC-MS/MS, we analyzed the total proteome alterations in these mice with each group having 5 biological replicates. The equivalent amount of liver protein in the IRI and IRI+EA groups was decreased, alkylated and digested through trypsin. Principle component analysis (PCA) of profiles of each specimen's protein expression revealed between each group, there were differences in the proteome's overall pattern. (Figure 3A). In total, 2724 proteins were detected with at least two unique peptides at a false discovery rate of < 1%. Then 338 proteins were selected as DEPs, with fold change > 2 and p < 0.05, including 73 DEPs being downregulated, and 265 DEPs were upregulated in the IRI+EA group than the IRI group (Figure 3B). The heatmap of DEPs was shown in Figure 3C. We then performed Gene Ontology analysis of DEPs. In the category of molecular functions, DEPs were significantly enriched in mRNA binding, ribonucleoprotein complex binding, organic acid binding, coenzyme binding, and lyase activity (Figure 3D). Biological processes enrichment analysis demonstrated that RNA processing-related processes including mRNA processing, RNA splicing, and ribonucleoprotein complex biogenesis were mainly enriched (Figure 3E). Other highly enriched biological processes included controlling translation and reactive oxygen species metabolic system. Notably, we observed that the cell survival and production of reactive oxygen species functions were highly enriched by IPA analysis, suggesting anti-oxidative stress caused cell death was closely related to electroacupuncture action (Figure 3F). The heat map showed the DEPs associated with the creation of reactive oxygen species (Figure 3G). We predicted the upstream regulators based on the DEPs (Supplemental Table 1) and built a DEPs-upstream regulators-biological processes network using IPA, which revealed that NFE2L2 (also known as Nrf2), a key regulator of oxidative stress, mediated cell survival was activated by EA stimulation (Figure 3H).

EA Stimulation on the ST36 Ameliorated Oxidative Stress Injury in Mice Hepatic IRI Through Activating Nrf2

To validate the impact of EA on oxidative stress in mouse hepatic IRI. We evaluated the oxidative/anti-oxidative status by detecting the MDA and SOD levels. As expected, EA administration decreased the MDA content and raised the SOD level than the IRI group (Figure 4A and B), indicating the anti-oxidative stress effect of EA. We then detected the effect of EA on the activation of the Nrf2 pathway. The expression of Nrf2 and its downstream genes HO-1 and NQO-1 were significantly added in the EA group than the IRI group (Figure 4C, F and G). Furthermore, EA administration promoted nuclear localization of Nrf2, leading to the higher expression of HO-1 and NQO-1 (Figure 4D and E). The results collectively demonstrated that EA administration on the ST36 ameliorated oxidative stress injury in mice hepatic IRI via activating the Nrf2 pathway.

Nrf2 Pathway Blockade Eliminated the Protective Action of EA on Hepatic IRI

To further verify the effect of EA on hepatic IRI depending on Nrf2 activation, the Nrf2 inhibitor ML385 was utilized in EA-treated hepatic IRI mice. ML385 was given intraperitoneally 1 hour before liver ischemia administration. The experimental design was shown in Figure 5A. As expected, ML385 treatment aggravated liver injury of IRI and blocked the hepatic protective effect of EA stimulation (Figure 5B–F). We then evaluated the activation of the Nrf2 pathway. The
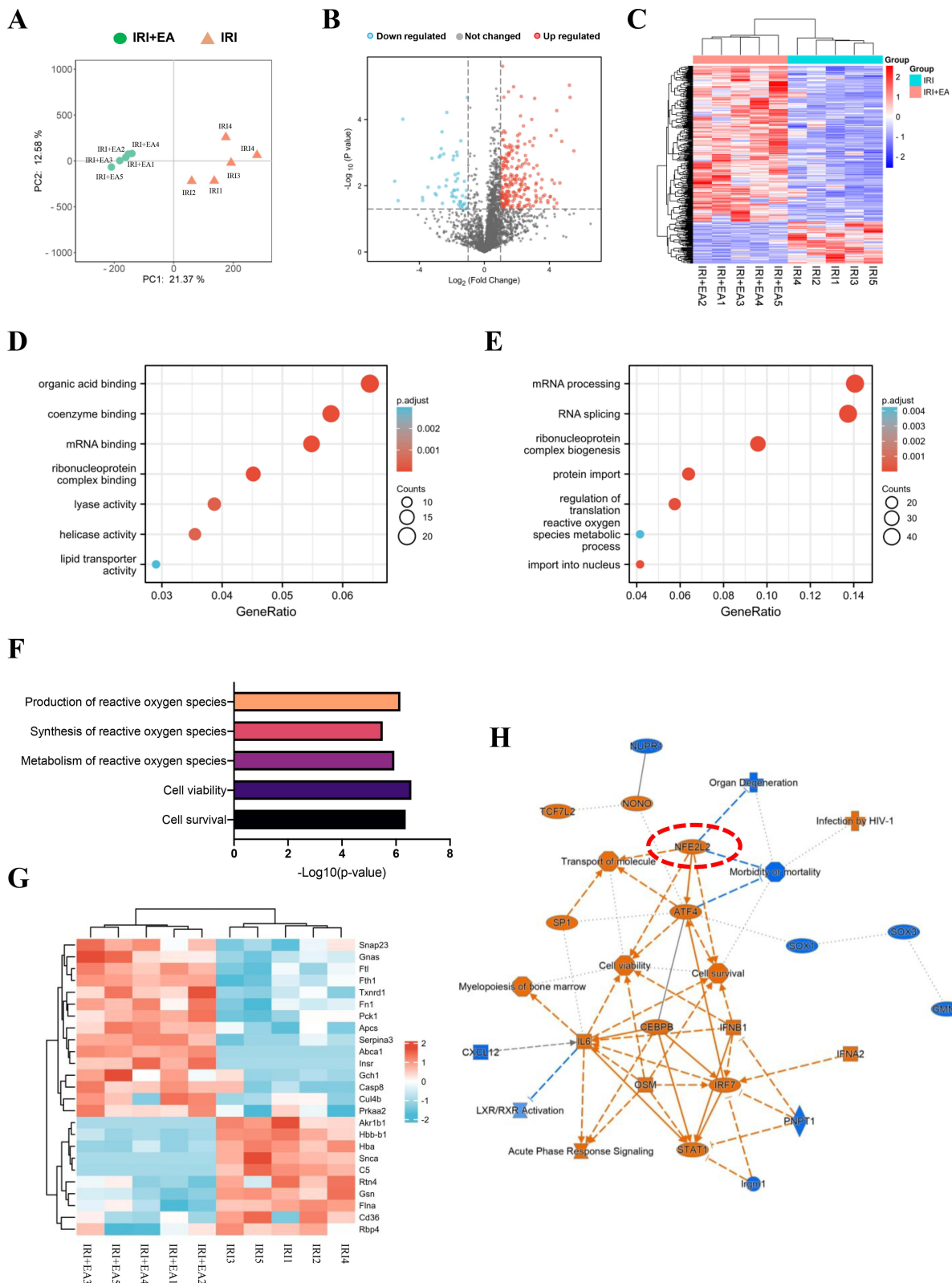
Figure 3 Quantitative proteomics analysis of livers after IRI. (**A**) Principle component analysis (PCA) of profiles of each specimen's protein expression revealed between each group. (**B**) Volcano plot of DEPs. (**C**) Heatmap of DEPs. (**D–F**) The molecular functions and biological processes enrichment analysis of DEPs. (**G**) The DEPs involved in the production of reactive oxygen species. (**H**) DEPs-upstream regulators-biological processes interaction network constructed by IPA.
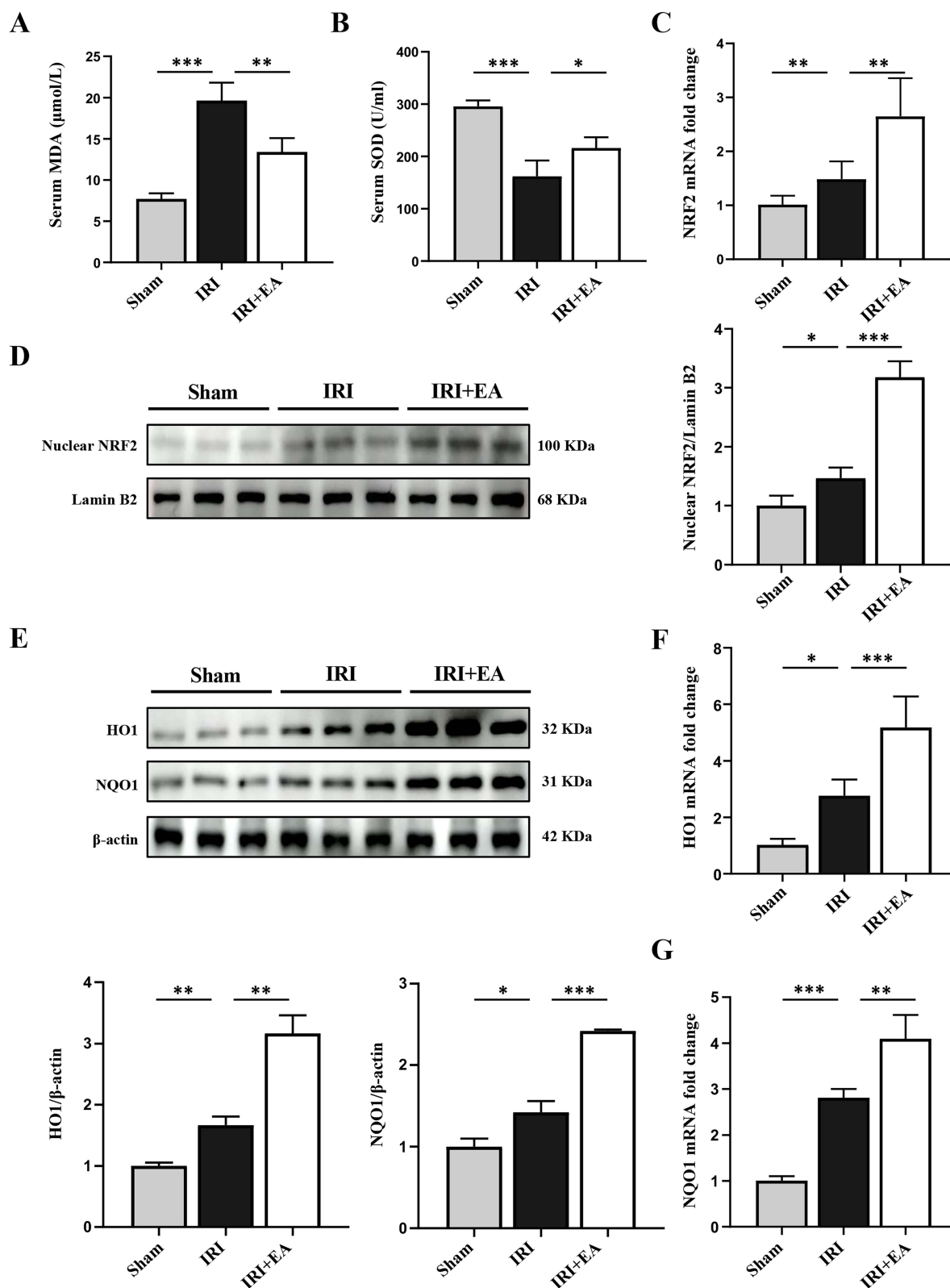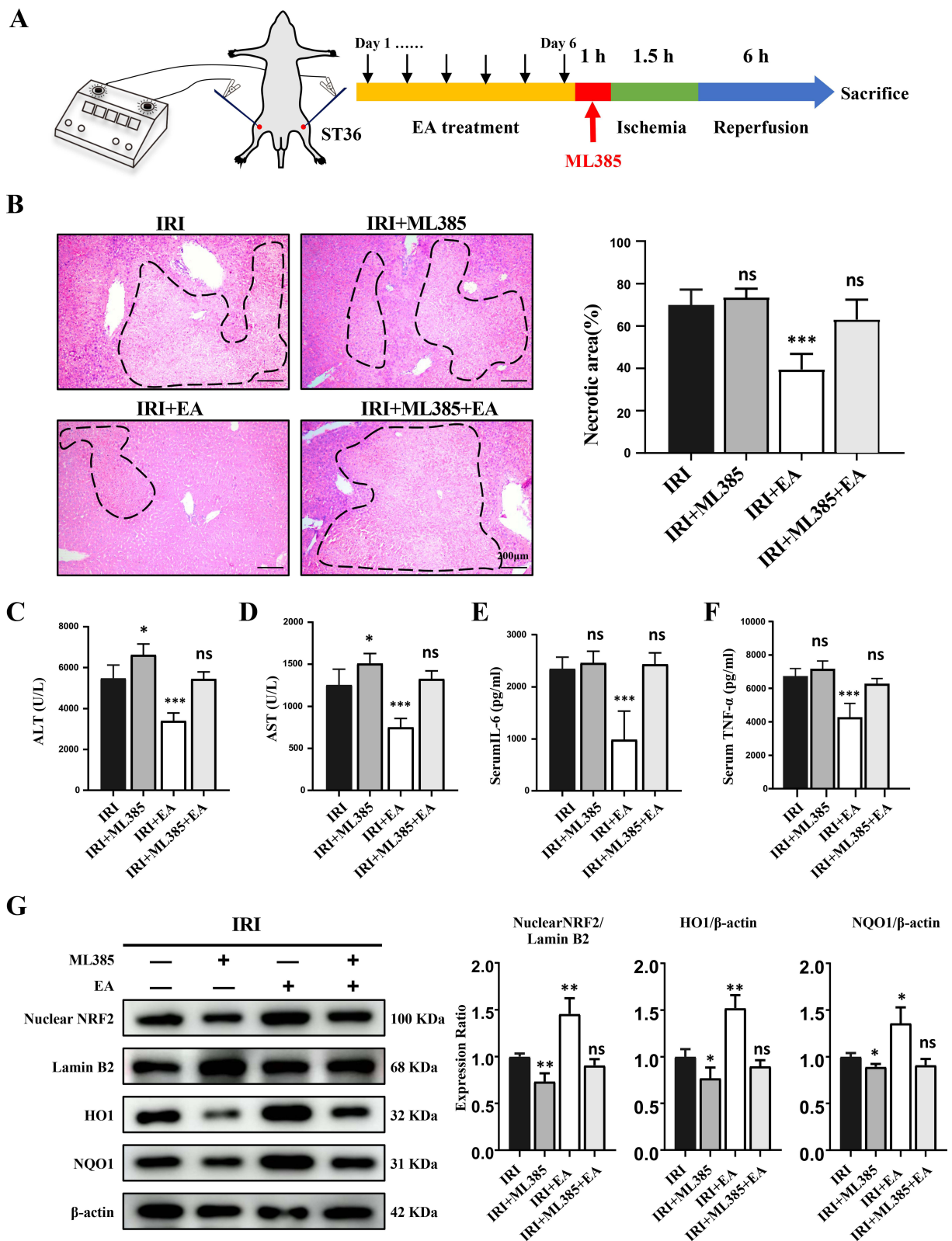
Figure 4 EA activated the Nrf2 pathway in mice hepatic IRI. (**A** and **B**) Serum MDA and SOD levels. (**C** and **D**) The mRNA and protein levels of Nrf2. (**E**–**G**) HO-1, NQO1 expression in the liver tissues. Lamin B and β-actin were used as loading controls. All data were presented as the mean ± SD. *P <0.05, **P < 0.01, ***P < 0.001 (n=3–5 per group).

Figure 5 ML385 reversed the protective impact of EA on liver IRI. (**A**) The experimental design. (**B**) H&E staining images of liver tissues (original magnification, × 100) showed necrotic areas. (**C** and **D**) ALT and AST levels in serum. (**E** and **F**) Serum levels of indicated cytokines. (**G**) Nuclear Nrf2, HO-1 and NQO1 expression in the liver tissues. Lamin B and β-actin were used as loading controls. All data were presented as the mean ± SD. *P <0.05, **P < 0.01, ***P < 0.001 (n=3–5 per group).

protein expression of Nrf2 nucleoprotein, total HO-1 and NQO-1 was largely decreased in the ML385+IRI group than the IRI group (Figure 5G). What's more, the protein expression of Nrf2 nucleoprotein, total HO-1 and NQO-1 protein in the IRI+ ML385+EA group was also dramatically decreased than the IRI+EA group. The results indicated that the EA attenuates the hepatic injury induced by IRI relying on the Nrf2 signal pathway.

Vagotomy Eliminated the Protective Action of EA on Liver IRI

Some studies have indicated that acupuncture at ST36 can activate the vagus nerve.[31] The left vagus nerve enters the abdominal cavity through the esophageal foramen to form the anterior vagus nerve trunk, which then branches directly into the liver. To check whether vagus nerve activation is necessary for the protective effects of EA on hepatic IRI, we cut the vagus nerve on the left side of the neck of mice 3 days before EA treatment (Figure 6A). We observed that mice underwent vagotomy aggravated liver injury of IRI, and inhibited the hepatic protective function of EA treatment (Figure 6B–F). The protein expression of Nrf2 nucleoprotein, total HO-1 and NQO-1 in the IRI+VNX group reduced greatly than the IRI group (Figure 6G). However, the protein expression of Nrf2 nucleoprotein, total HO-1 and NQO-1 in the IRI+VNX+EA group was highly decreased than the IRI+EA group. The results collectively demonstrated that the intact vagus nerve is essential to the function of EA on hepatic IRI.

Discussion

Our research evaluated the effect of EA at ST36 on hepatic IRI by employing an IRI mouse model. We observed that EA pretreatment significantly alleviated necrotic areas and downregulated proinflammatory cytokines in the liver tissue caused by hepatic ischemia/reperfusion (Figures 1D and 2A–F). To understand how EA affects hepatic IRI, we also used a label-free quantitative proteomics technique to profile the proteome of liver tissues. The analysis of DEPs showed that the treatment against IRI by electroacupuncture of ST36 was mainly associated with its anti-oxidative stress response through activation of the Nrf2 pathway, which was then validated in vivo. The effect of EA was eliminated when we used ML385, an inhibitor of Nrf2 and vagotomy. The data demonstrated that EA at ST36 could relieve hepatic inflammation responses and cell death by regulating Nrf2-mediated oxidative stress response through the vagus nerve.

Inflammatory response plays a crucial role in IRI. NF-κB is a component of cellular responses to stimuli and is widely present in the animal cell. As we all know that NF-κB transcriptionally regulates a range of potentially pro-inflammatory, inflammatory, stress and growth-responsive genes. It has been shown that EA can inactivate the NF-κB signal to reduce the inflammatory reaction in several disease settings.[32] Consistent with previous studies, the protein level of IκBα, which inhibits inflammation, was notably upregulated in the EA group. Moreover, p-NF-κb and p-IκBα levels, which induce inflammation, were decreased.

Surgery is the usual treatment option for patients with advanced liver disease such as liver cancer or cirrhosis. However, the success of such protocols is often hampered by the damage caused by IRI. In multiple animal models of hepatic IRI, ROS and oxidative stress are very important disease injury mechanisms which occur in the early stage of reperfusion.[33] With the increased macrophages and neutrophils infiltration, ROS is further released, leading to cellular damage. This was consistent with our finding that liver infiltration of neutrophils and macrophages was largely increased in IRI model mice, besides the levels of oxidative stress had risen (Figures 2G and 4A). Therefore, further improving our understanding of hepatic inflammation and oxidative stress is necessary. In addition, more improved anti-inflammatory and antioxidant strategies need to be developed and tested. The EA provides a feasible opportunity to achieve safe and effective interventions.

Mass spectrometry-based proteomics discovery provides a powerful tool for identifying and quantifying large-scale protein profiles for the discovery of disease-related proteins and signaling pathways. In the present study, 338 DEPs were identified between the IRI group and the IRI+EA group. Bioinformatic analysis of molecular functions and biological processes of DEPs were significantly enriched in RNA metabolism and processing-related processes, as well as the mRNA-binding function. We, therefore, hypothesized that gene expression regulation of EA was mainly mediated by post-transcriptional regulation (Figure 3D and E). Through IPA analysis, we found that the oxidative stress process and its regulator Nrf2 were closely related to EA treatment. After ROS attack, Nrf2 separates from Keap1, enters into the nucleus, and links to antioxidant response elements, thereby regulating various antioxidant gene levels, such as SOD,
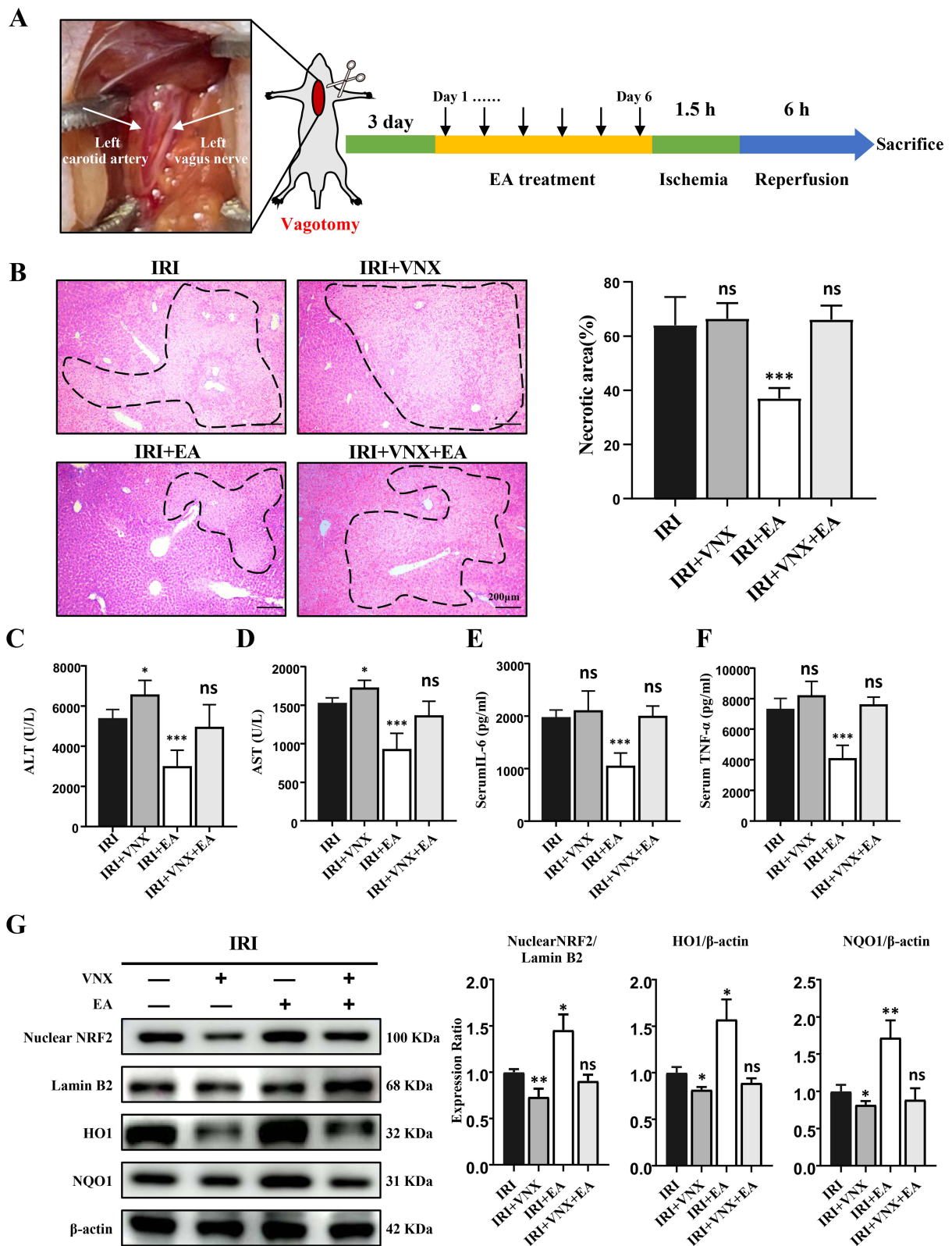
Figure 6 Vagotomy eliminated the protective action of EA on liver IRI and inhibits the Nrf2 pathway. (**A**) Display of the left vagus nerve and the experimental design. (**B**) H&E staining images of liver tissues (original magnification, × 100) showed necrotic areas. (**C** and **D**) Serum levels of ALT and AST. (**E** and **F**) Serum levels of indicated cytokines. (**G**) Nuclear Nrf2, HO-1 and NQO1 expression in the liver tissues. Lamin B and β-actin were used as loading controls. All data were presented as the mean ± SD. *P <0.05, **P < 0.01, ***P < 0.001 (n=3–5 per group).

HO-1, and NQO1, which are necessary for maintaining cellular redox homeostasis. Nrf2 mediates the expression of a variety of endogenous antioxidants and plays an important function in cellular resistance to oxidative stress. Nrf2-deficient mice are more susceptible to multiple causes of induced liver injury,[18,34,35] suggesting that Nrf2 protects hepatocytes through multiple cellular pathways. In studies of hepatic IRI, Nrf2 can activate a phosphatidylinositol-3-kinase/AKT pathway,[36] apoptotic/necroptotic cell death pathway,[37] and other signaling pathways to protect the liver. EA has been shown to activate Nrf2.[38] However, the mechanism by which EA is involved in liver disease has rarely been reported. As expected, our validation results using an Nrf2 inhibitor showed that Nrf2 inhibition counteracted the therapeutic effect of EA and exacerbated the inflammatory responses caused by IRI. In our study, we found that Nrf2 might protect hepatocytes by inhibiting inflammation and oxidative stress. The results demonstrated that Nrf2 signaling was the crucial pathway for EA in hepatic protection.

The vagus nerve (a complex mixed nerve) is the tenth cerebral nerve with a close connection to the EA. As a complex neural network, the vagus nerve maintains the mental and physical balance of our body. The electrical intervention of the vagus nerve significantly attenuates the inflammatory action and alleviates the severity of illness in the models of endotoxemia, sepsis, and some inflammatory animal models.[39] The study demonstrated that vagus nerve stimulation could activate the Nrf2/HO-1 pathway.[1] Our experiment observed that the activation of Nrf2 by EA in IRI was also related to the vagus nerve in mice, and vagotomy inhibited the effectiveness of EA treatment.

Conclusion

In conclusion, our study has demonstrated that EA pretreatment at ST36 significantly ameliorates hepatic IRI in mice by inhibiting oxidative stress via activating the Nrf2 signal pathway, which was vagus nerve-dependent.

Abbreviations

IRI, Ischemia/Reperfusion Injury; EA, electroacupuncture; SEA, acupuncture without electrical stimulation; NAcuP, none acupoint; ST36, Zusanli; ALT, alanine aminotransferase; AST, aspartate aminotransferase; H&E, hematoxylin-eosin staining; IL-6, Interleukin-6; TNF-α, Tumor necrosis factor-α; IL-1β, Interleukin-1β; MPO, myeloperoxidase; NF-κb, nuclear factor kappa-B; IκBα, inhibitor of NF-κB; IHC, immunohistochemistry; Nrf2, nuclear factor erythroid-2 related factor 2; HO-1, Heme Oxygenase-1; NQO-1, NAD(P)H, quinone oxidoreductase 1; MDA, malondialdehyde; SOD, superoxide dismutase; VNX, vagotomy; qRT-PCR, quantitative real-time polymerase chain reaction; VNS, Vagus nerve stimulation; IPA, ingenious pathway analysis; LC-MS/MS, Liquid chromatography-tandem mass spectrometry; IPA, ingenious pathway analysis.

Acknowledgments

Author Contributions

All authors made a significant contribution to the work reported, whether that is in the conception, study design, execution, acquisition of data, analysis and interpretation, or in all these areas; took part in drafting, revising or critically reviewing the article; gave final approval of the version to be published; have agreed on the journal to which the article has been submitted; and agree to be accountable for all aspects of the work.

Funding

Disclosure

The authors declare no competing interests in this work.

References

1. Zhang Q, Lai Y, Deng J, et al. Vagus nerve stimulation attenuates hepatic ischemia/reperfusion injury via the Nrf2/HO-1 pathway. *Oxid Med Cell Longev*. 2019;2019:9549506. doi:10.1155/2019/9549506
2. Li C, Jackson RM. Reactive species mechanisms of cellular hypoxia-reoxygenation injury. *Am J Physiol Cell Physiol*. 2002;282(2):C227–41. doi:10.1152/ajpcell.00112.2001
3. Wu L, Xiong X, Wu X, et al. Targeting oxidative stress and inflammation to prevent ischemia-reperfusion injury. *Front Mol Neurosci*. 2020;13:28. doi:10.3389/fnmol.2020.00028
4. Xu D, Chen L, Chen X, et al. The triterpenoid CDDO-imidazolide ameliorates mouse liver ischemia-reperfusion injury through activating the Nrf2/HO-1 pathway enhanced autophagy. *Cell Death Dis*. 2017;8(8):e2983. doi:10.1038/cddis.2017.386
5. Xiao Y, Chen W, Zhong Z, et al. Electroacupuncture preconditioning attenuates myocardial ischemia-reperfusion injury by inhibiting mitophagy mediated by the mTORC1-ULK1-FUNDC1 pathway. *Biomed Pharmacother*. 2020;127:110148. doi:10.1016/j.biopha.2020.110148
6. Mei ZG, Huang YG, Feng ZT, et al. Electroacupuncture ameliorates cerebral ischemia/reperfusion injury by suppressing autophagy via the SIRT1-FOXO1 signaling pathway. *Aging*. 2020;12(13):13187–13205. doi:10.18632/aging.103420
7. Oh JE, Kim SN. Anti-inflammatory effects of acupuncture at ST36 point: a literature review in animal studies. *Front Immunol*. 2021;12:813748. doi:10.3389/fimmu.2021.813748
8. Geng Z, Nie X, Ling L, et al. Electroacupuncture may inhibit oxidative stress of premature ovarian failure mice by regulating intestinal microbiota. *Oxid Med Cell Longev*. 2022;2022:4362317. doi:10.1155/2022/4362317
9. Cahn AM, Carayon P, Hill C, Flamant R. Acupuncture in gastroscopy. *Lancet*. 1978;1(8057):182–183. doi:10.1016/s0140-6736(78)90614-1
10. Chen CY, Ke MD, Kuo CD, Huang CH, Hsueh YH, Chen JR. The influence of electro-acupuncture stimulation to female constipation patients. *Am J Chin Med*. 2013;41(2):301–313. doi:10.1142/s0192415x13500225
11. Zhu YJ, Wu XY, Wang W, et al. Acupuncture for quality of life in gastric cancer patients undergoing adjuvant chemotherapy. *J Pain Symptom Manage*. 2022;63(2):210–220. doi:10.1016/j.jpainsymman.2021.09.009
12. Jang JH, Yeom MJ, Ahn S, et al. Acupuncture inhibits neuroinflammation and gut microbial dysbiosis in a mouse model of Parkinson's disease. *Brain Behav Immun*. 2020;89:641–655. doi:10.1016/j.bbi.2020.08.015
13. Zhao H, Dong F, Li Y, et al. Inhibiting ATG5 mediated autophagy to regulate endoplasmic reticulum stress and CD4(+) T lymphocyte differentiation: mechanisms of acupuncture's effects on asthma. *Biomed Pharmacother*. 2021;142:112045. doi:10.1016/j.biopha.2021.112045
14. Huang CL, Tsai PS, Wang TY, Yan LP, Xu HZ, Huang CJ. Acupuncture stimulation of ST36 (Zusanli) attenuates acute renal but not hepatic injury in lipopolysaccharide-stimulated rats. *Anesth Analg*. 2007;104(3):646–654. doi:10.1213/01.ane.0000255288.68199.eb
15. Ucar BI, Ucar G, Saha S, Buttari B, Profumo E, Saso L. Pharmacological protection against ischemia-reperfusion injury by regulating the Nrf2-Keap1-ARE signaling pathway. *Antioxidants*. 2021;10(6). doi:10.3390/antiox10060823
16. Tonelli C, Chio IIC, Tuveson DA. Transcriptional regulation by Nrf2. *Antioxid Redox Signal*. 2018;29(17):1727–1745. doi:10.1089/ars.2017.7342
17. Tanaka N, Ikeda Y, Ohta Y, et al. Expression of Keap1-Nrf2 system and antioxidative proteins in mouse brain after transient middle cerebral artery occlusion. *Brain Res*. 2011;1370:246–253. doi:10.1016/j.brainres.2010.11.010
18. Thimmulappa RK, Lee H, Rangasamy T, et al. Nrf2 is a critical regulator of the innate immune response and survival during experimental sepsis. *J Clin Invest*. 2006;116(4):984–995. doi:10.1172/jci25790
19. Shih AY, Li P, Murphy TH. A small-molecule-inducible Nrf2-mediated antioxidant response provides effective prophylaxis against cerebral ischemia in vivo. *J Neurosci*. 2005;25(44):10321–10335. doi:10.1523/jneurosci.4014-05.2005
20. Liu M, Grigoryev DN, Crow MT, et al. Transcription factor Nrf2 is protective during ischemic and nephrotoxic acute kidney injury in mice. *Kidney Int*. 2009;76(3):277–285. doi:10.1038/ki.2009.157
21. Zhang Y, Sano M, Shinmura K, et al. 4-hydroxy-2-nonenal protects against cardiac ischemia-reperfusion injury via the Nrf2-dependent pathway. *J Mol Cell Cardiol*. 2010;49(4):576–586. doi:10.1016/j.yjmcc.2010.05.011
22. Fonseca RC, Bassi GS, Brito CC, et al. Vagus nerve regulates the phagocytic and secretory activity of resident macrophages in the liver. *Brain Behav Immun*. 2019;81:444–454. doi:10.1016/j.bbi.2019.06.041
23. Izumi T, Imai J, Yamamoto J, et al. Vagus-macrophage-hepatocyte link promotes post-injury liver regeneration and whole-body survival through hepatic FoxM1 activation. *Nat Commun*. 2018;9(1):5300. doi:10.1038/s41467-018-07747-0
24. Han J-S. Acupuncture: neuropeptide release produced by electrical stimulation of different frequencies. *Trends Neurosci*. 2003;26:17–22. doi:10.1016/s0166-2236(02)00006-1
25. Xu M, Hang H, Huang M, et al. DJ-1 deficiency in hepatocytes improves liver ischemia-reperfusion injury by enhancing mitophagy. *Cell Mol Gastroenterol Hepatol*. 2021;12(2):567–584. doi:10.1016/j.jcmgh.2021.03.007
26. Jiao J, Jiang Y, Qian Y, et al. Expression of STING is increased in monocyte-derived macrophages and contributes to liver inflammation in hepatic ischemia-reperfusion injury. *Am J Pathol*. 2022. doi:10.1016/j.ajpath.2022.09.002
27. Zhi S, Congcong Z, Zhiling G, et al. Quantitative proteomics of HFD-induced fatty liver uncovers novel transcription factors of lipid metabolism. *Int J Biol Sci*. 2022;18(8):3298–3312. doi:10.7150/ijbs.71431
28. Zhang T, Yang WX, Wang YL, et al. Electroacupuncture preconditioning attenuates acute myocardial ischemia injury through inhibiting NLRP3 inflammasome activation in mice. *Life Sci*. 2020;248:117451. doi:10.1016/j.lfs.2020.117451
29. Wen J, Chen X, Yang Y, et al. Acupuncture medical therapy and its underlying mechanisms: a systematic review. *Am J Chin Med*. 2021;49(1):1–23. doi:10.1142/S0192415X21500014
30. Bardallo GR, Panisello-Roselló A, Sanchez-Nuno S, et al. Nrf2 and oxidative stress in liver ischemia/reperfusion injury. *FEBS J*. 2022;289(18):5463–5479. doi:10.1111/febs.16336
31. Lu MJ, Yu Z, He Y, Yin Y, Xu B. Electroacupuncture at ST36 modulates gastric motility via vagovagal and sympathetic reflexes in rats. *World J Gastroenterol*. 2019;25(19):2315–2326. doi:10.3748/wjg.v25.i19.2315

32. Gusmao J, Fonseca KM, Ferreira BSP, et al. Electroacupuncture reduces inflammation but not bone loss on periodontitis in arthritic rats. *Inflammation*. 2021;44(1):116–128. doi:10.1007/s10753-020-01313-x

33. Jaeschke H, Woolbright BL. Current strategies to minimize hepatic ischemia-reperfusion injury by targeting reactive oxygen species. *Transplant Rev*. 2012;26(2):103–114. doi:10.1016/j.trre.2011.10.006

34. Enomoto A, Itoh K, Nagayoshi E, et al. High sensitivity of Nrf2 knockout mice to Acetaminophen hepatotoxicity associated with decreased expression of ARE-regulated drug metabolizing enzymes and antioxidant genes. *Toxicol Sci*. 2001;59(1):169–177. doi:10.1093/toxsci/59.1.169

35. Zhang YK, Yeager RL, Tanaka Y, Klaassen CD. Enhanced expression of Nrf2 in mice attenuates the fatty liver produced by a methionine- and choline-deficient diet. *Toxicol Appl Pharmacol*. 2010;245(3):326–334. doi:10.1016/j.taap.2010.03.016

36. Li S, Zhu Z, Xue M, et al. The protective effects of fibroblast growth factor 10 against hepatic ischemia-reperfusion injury in mice. *Redox Biol*. 2021;40:101859. doi:10.1016/j.redox.2021.101859

37. Zhan Y, Xu D, Tian Y, et al. Novel role of macrophage TXNIP-mediated CYLD-NRF2-OASL1 axis in stress-induced liver inflammation and cell death. *JHEP Rep*. 2022;4(9):100532. doi:10.1016/j.jhepr.2022.100532

38. Yu JB, Shi J, Gong LR, et al. Role of Nrf2/ARE pathway in protective effect of electroacupuncture against endotoxic shock-induced acute lung injury in rabbits. *PLoS One*. 2014;9(8):e104924. doi:10.1371/journal.pone.0104924

39. Borovikova LV, Ivanova S, Zhang M, et al. Vagus nerve stimulation attenuates the systemic inflammatory response to endotoxin. *Nature*. 2000;405 (6785):458–462. doi:10.1038/35013070